# NATIONAL ADVISORY COMMITTEE FOR AERONAUTICS

TECHNICAL NOTE 2534

EXPERIMENTAL INVESTIGATION OF THE LOW-SPEED STATIC AND YAWING STABILITY CHARACTERISTICS OF A 45° SWEPTBACK HIGH-WING CONFIGURATION WITH VARIOUS

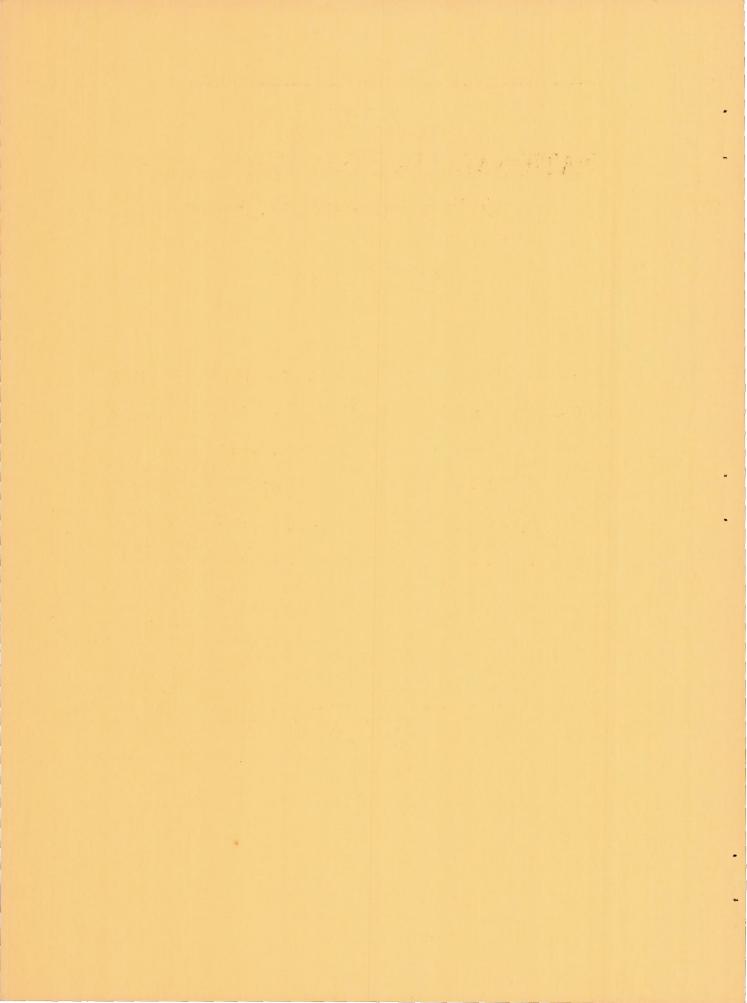
TWIN VERTICAL WING FINS

By Alex Goodman and Walter D. Wolhart

Langley Aeronautical Laboratory
Langley Field, Va.



Washington November 1951



# TECHNICAL NOTE 2534

EXPERIMENTAL INVESTIGATION OF THE LOW-SPEED STATIC AND YAWING STABILITY CHARACTERISTICS OF A 45° SWEPTBACK HIGH-WING CONFIGURATION WITH VARIOUS

TWIN VERTICAL WING FINS

By Alex Goodman and Walter D. Wolhart

## SUMMARY

An investigation was made to determine the low-speed static stability and yawing stability characteristics of a 45° sweptback high-wing, lowhorizontal-tail configuration with various twin vertical wing fins. In general, the static longitudinal stability characteristics were not affected by either upper-surface or lower-surface wing fins. The results indicated that the directional stability for a high-wing configuration with twin upper-surface or lower-surface vertical fins located at 70 percent of the wing semispan was smaller at low angles of attack than for a similar configuration with only a single vertical tail at the rear of the fuselage. The twin-fin configurations, however, were directionally stable throughout the angle-of-attack range, whereas the single verticaltail configuration was directionally unstable at moderate and high angles of attack. The twin upper-surface fin configuration was found to be more directionally stable at low angles of attack but only 50 percent as effective as the twin lower-surface fin configuration at moderate angles of attack. At high angles of attack, the directional stability for the upper-surface fin configuration decreased as the angle of attack increased. The positive effective dihedral (at 00 angle of attack) normally associated with a high-wing fuselage configuration was increased by the addition of twin lower-surface wing fins at 70 percent of the wing semispan. As the lower-surface fins were moved outboard, the effective dihedral was reduced. In the case of the upper-surface wing fins, the effective dihedral of the complete configuration was made more positive throughout the angle-of-attack range.

The yawing stability characteristics obtained with the upper-surface or lower-surface fin configurations were approximately the same at low angles of attack. At the higher angles of attack, however, the damping in yaw contributed by the upper-surface fins tended to decrease as the angle of attack was increased.

# INTRODUCTION

Requirements for satisfactory high-speed performance of aircraft have resulted in configurations that differ in many respects from previous designs. As a result of these changes, the designer has little assurance that the low-speed characteristics will be satisfactory for any specific configuration. The low-speed characteristics of wings suitable for high-speed flight have been investigated quite extensively. The contribution of other components of the aircraft, or of various combinations of components, however, are not well-understood. In order to provide such information, a series of investigations of models having various interchangeable components is being conducted in the Langley stability tunnel.

Results from two investigations made in the Langley stability tunnel have indicated that the optimum configuration tested with regard to static longitudinal stability would be a high-wing model with the horizontal tail located below the wing chord plane (references 1 and 2). It has also been shown, however, that for a high-wing model a strong sidewash is produced at the plane of symmetry because of the wing-fuselage interference (references 2 and 3). For configurations with the vertical tail located on the fuselage, this sidewash reduces the vertical-tail contribution to the directional stability. At moderate and high angles of attack a further reduction in the directional stability results. This reduction at high angles of attack may be attributed to an additional unfavorable sidewash at the vertical tail which results from the lateral movement of the wing-tip vortices (reference 2). Consideration of the results of references 1 and 2 indicated that an airplane configuration might have both longitudinal and directional stability over a large range of angles of attack if it had a high wing, a low horizontal tail, and the vertical-fin area in a region of less adverse sidewash. The present investigation, therefore, was made to determine the static-stability and yawing-stability derivatives of a 45° sweptback high-wing, lowhorizontal-tail model with vertical fins located on the wing.

## SYMBOLS

The data are presented in the form of standard NACA coefficients of forces and moments which are referred to the stability system of axes, with the origin at the projection on the plane of symmetry of the quarter-chord point of the mean aerodynamic chord of the wing. The positive directions of the forces, moments, and angular displacements are shown in figure 1. The coefficients and symbols are defined as follows:

C<sub>T.</sub> lift coefficient (L/qSW)

 $C_m$  pitching-moment coefficient  $(M/qS_W\overline{c}_W)$ 

$C_{\mathbf{Y}}$	lateral-force	coefficient	(Y/c	(SW)
------------------	---------------	-------------	------	------

$$C_n$$
 yawing-moment coefficient  $(N/qS_Wb_W)$ 

q free-stream dynamic pressure, pounds per square foot 
$$(\rho V^2/2)$$

mean aerodynamic chord, feet 
$$\left(\frac{2}{5}\int_{0}^{b/2}c^{2}dy\right)$$

$$\left(\frac{2}{5}\int_0^{b/2} cx dy\right)$$

- Z<sub>H</sub> horizontal-tail height, perpendicular distance from fuselage center line to horizontal-tail chord plane, feet
- tail or fin length, distance parallel to fuselage center line from origin of axes to  $\overline{c}/4$  of tail or fins, feet
- y distance measured perpendicular to plane of symmetry, feet
- d maximum diameter of fuselage, feet

$$\lambda$$
 taper ratio  $\left(\frac{\text{Tip chord}}{\text{Root chord}}\right)$ 

- angle of attack, degrees
- $\psi$  angle of yaw, degrees (for force tests,  $\psi = -\beta$ )
- β angle of sideslip, degrees
- r yawing angular velocity, radians per second
- rb
  2V yawing-velocity parameter, radians

$$C_{m_{\alpha}} = \frac{\partial C_{m}}{\partial \alpha}$$
, per degree

$$C_{Y_{\psi}} = \frac{\partial C_{Y}}{\partial \psi}$$
, per degree

$$C_{l\psi} = \frac{\partial C_l}{\partial \psi}$$
, per degree

$$C_{n_{\psi}} = \frac{\partial C_n}{\partial \psi}$$
, per degree

$$C_{Y_r} = \frac{\partial C_Y}{\partial \left(\frac{rb}{2V}\right)}$$
, per radian

$$C_{l_r} = \frac{\partial C_l}{\partial \left(\frac{rb}{2V}\right)}$$
, per radian

$$C_{n_r} = \frac{\partial C_n}{\partial \left(\frac{rb}{2V}\right)}$$
, per radian

5

Subscripts and abbreviations:

W<sub>1</sub>, W<sub>2</sub>, W<sub>3</sub> wing positions

F fuselage

H<sub>1</sub>, H<sub>2</sub>, H<sub>3</sub> horizontal-tail positions

V vertical tail

v rear vertical fin (see fig. 2)

f<sub>1</sub> basic fin (see fig. 2)

f<sub>2</sub> modified fin (see fig. 2)

#### APPARATUS AND MODELS

The tests of the present investigation were conducted in the 6- by 6-foot test section of the Langley stability tunnel. In this section curved flight can also be simulated by causing air to flow in a curved path about a fixed model.

The swept-wing general research model of reference 2 was employed for these tests. Plan and elevation views of the complete model showing the wing, horizontal tail, and fin positions are presented in figure 2. A list of the pertinent geometric characteristics of the various component parts is given in table I. All components of the model were constructed of mahogany.

The fuselage was a body of revolution (fineness ratio of 6.90) having a circular-arc profile with a blunt tail end. The wing and horizontal tail had an aspect ratio of 4.0, a taper ratio of 0.6, and an NACA 65A008 profile in sections parallel to the plane of symmetry. The quarter-chord lines were swept back 45°. Ordinates for the NACA 65A008 airfoil section and for the fuselage are given in tables II and III, respectively. The twin lower-surface fins tested  $f_1$  and  $f_2$  had aspect ratios of 1.2 and 1.7, respectively. These fins had flat-plate profiles with round leading edges and beveled trailing edges. The small rear vertical fin v was triangular in plan form and had an aspect ratio of 0.84.

The model was mounted on a single strut at the origin of the axes shown in figure 2. Forces and moments were measured by means of a

six-component balance system. Photographs of two of the model configurations tested are presented as figure 3. All lifting surfaces were set at  $0^{\circ}$  incidence with respect to the fuselage center lines.

#### TESTS

The tests in straight flow were made at a dynamic pressure of 39.8 pounds per square foot which corresponds to a Mach number of about 0.17 and a Reynolds number of  $0.88 \times 10^6$  based on the mean aerodynamic chord of the wing. In yawing flow, the tests were made at a dynamic pressure of 24.9 pounds per square foot which corresponds to a Mach number of about 0.13 and a Reynolds number of  $0.71 \times 10^6$  based on the mean aerodynamic chord of the wing.

In straight flow, the static longitudinal and lateral stability characteristics were obtained from tests of the model at angles of yaw of 0° and ±5°. The yawing stability characteristics were obtained from tests of the model at values of rb/2V of 0, -0.0311, -0.0660, and -0.0870.

The angle-of-attack range for all tests was from about -2° up to about 30°.

#### CORRECTIONS

Approximate corrections, based on unswept-wing theory, for the effects of jet boundaries have been applied to the angle of attack (reference 4). The data have also been corrected for the effects of blocking (reference 5). Corrections for the effects of support-strut interference have not been applied since the forces obtained for a similar model in reference 2 were found to be small.

The lateral force due to yawing has been corrected for the effects of the static-pressure gradient associated with curved flow.

#### RESULTS AND DISCUSSION

#### Presentation of Results and General Remarks

Some of the results illustrating the static-stability difficulties discussed in the introduction are given in figure 4 and were taken from reference 2.

As indicated in figure 4, a 45° sweptback low-wing, high-horizontal-tail configuration ( $W_3$  + F + V +  $W_2$ , in fig. 2) has an unstable  $C_{m\alpha}$  variation at moderate angles of attack because the horizontal tail is in a strong downwash field (see references 1 and 2). This configuration, however, has good directional stability throughout the angle-of-attack range because of the favorable sidewash at the vertical tail caused by the wing-fuselage interference. (See references 2 and 3.) On the other hand, a 45° sweptback high-wing, low-horizontal-tail configuration ( $W_2$  + F + V +  $W_1$ , in fig. 2) has good longitudinal stability characteristics because the horizontal tail is below the wing wake for most of the angle-of-attack range. This configuration, however, becomes directionally unstable at moderate and high angles of attack because of an unfavorable sidewash at the vertical tail (references 2 and 3).

A high-wing, low-horizontal-tail arrangement which is desirable for longitudinal stability makes possible the repositioning of the vertical fin area from the rear of the fuselage to a region of less adverse sidewash; namely, the surface of the wing. The present investigation was, therefore, made to determine the static-stability and yawing-stability derivatives of a 45° sweptback high-wing, low-horizontal-tail model with vertical fins located on the wing.

The data obtained during the present investigation are given as curves of the static longitudinal and lateral stability characteristics (figs. 5 to 7) and yawing characteristics (fig. 8) plotted against angle of attack for the model with various fin arrangements.

# Static Stability Characteristics

Basic configurations without vertical fins.— For practical consideration, the  $45^{\circ}$  sweptback high-wing, low-horizontal-tail configuration  $W_2 + F + V + H_1$  of reference 2 was modified so that the horizontal tail was located above the hypothetical jet axis but still below the wing chord plane. This resulted in the basic configuration  $W_2 + F + H_3$  of the present paper. (See fig. 2.) However, the basic configuration  $W_2 + F + H_3$  was still longitudinally stable throughout the angle-of-attack range (figs. 4 and 5) as might be expected from the relative position of the wing and horizontal tail (references 1 and 2).

As pointed out in references 2 and 3, a high-wing configuration will have a positive effective dihedral  $C_{l\psi}$  at  $0^{\circ}$  angle of attack because of the wing-fuselage interference. A physical picture indicating the cause of this effect is presented in figure 9(a). The directional

instability of the basic configuration (positive  $C_{n\psi}$ ) is attributable to the unstable yawing moment associated with fuselages (reference 6).

Basic configuration with twin lower-surface fins .- The twin vertical fins fl were tested on the lower surface of the wing at 0.70b/2 and 0.98b/2. The addition of the twin lower-surface fins to the basic configuration at either station had no appreciable effect on the longitudinal characteristics (fig. 5). The main effect of adding the twin lower-surface fins at either station was to make the complete configuration W2 + F + H3 + f1 directionally stable throughout the angle-ofattack range. The fins at 0.98b/2 contributed a larger stabilizing increment in  $C_{n,k}$  than did the inboard fins at 0.70b/2 because of the longer tail length (fig. 2). The contribution of the twin lower-surface fin configurations to the directional stability parameter Cny was small at low angles of attack in comparison with the contribution of the singlevertical-tail configuration of reference 2. (Compare figs. 4 and 5.) However,  $C_{n_{\psi}}$  for the high-wing, single-vertical-tail configuration of reference 2 reversed sign (the configuration became directionally unstable) at moderate angles of attack; whereas, the twin lower-surface fin configuration was directionally stable throughout the angle-of-attack range.

The spanwise position of the twin lower-surface fins had a marked effect on the effective-dihedral parameter Clu at 00 angle of attack. With the twin lower-surface fins located at 0.70b/2, the antisymmetric loading induced on the wing at 0° angle of attack increased the effective dihedral. As the fins were moved outboard, the antisymmetric loading induced by the twin lower-surface fins on the wing reduced the positive effective dihedral. With the fins located at 0.98b/2, the induced loading apparently was large enough to cancel the positive effective dihedral caused by wing-fuselage interference (fig. 5). A representation is given in figure 9(b) of the spanwise load distribution over the wing as affected by the wing-fuselage interference and the wing-fin interference. Although consideration of figure 9(b) will not indicate whether the increment in  $C_{l\psi}$  caused by addition of the twin lower-surface fins will be positive or negative for all spanwise positions of the fins, it does indicate the direction in which Clour will change with a change in spanwise position of the fins.

Basic configuration with twin upper-surface fins. The twin lower-surface fin configurations were directionally stable throughout the angle-of-attack range but to a lesser degree at low angles of attack than the single-vertical-tail configuration of reference 2. Since

the 0.70b/2 location of the twin lower-surface fins appeared to be reasonable from structural considerations, an attempt was made to improve the stability of this configuration by adding a small amount of fin area above the wing surface to form fin  $f_2$ . Only a small improvement was obtained in the directional stability (figs. 5 and 6). None of the other parameters were affected appreciably except for a small increase in longitudinal stability at moderate angles of attack.

The twin upper-surface fin configuration  $W_2 + F + H_3 + f_1$  at 0.70b/2 also had good longitudinal stability throughout the angle-of-attack range (fig. 6). The longitudinal stability for the moderate angle-of-attack range was better (more negative  $C_{m_{\rm CL}}$ ) than had been obtained with the other twin-fin arrangements tested. This increase in longitudinal stability may be attributed to the fact that the twin upper-surface fins might have delayed the normal inboard movement of the wing-tip vortices with an increase in angle of attack. This delay in the inboard movement of the wing-tip vortices would have caused the horizontal tail to operate in a less unfavorable downwash field.

The twin upper-surface fin configuration was directionally stable (negative  $C_{n_{\psi}}$ ) throughout the angle-of-attack range. The variation of  $C_{n_{\psi}}$  with angle of attack was nearly constant for this configuration.

At 0° angle of attack, a more negative value of  $C_{n_{\psi}}$  was obtained with the upper-surface fin configuration than was obtained with the lower-surface fin configuration (compare figs. 5 and 6). This negative increase in  $C_{n_{\psi}}$  can be accounted for by considering the effects on the fins of the induced antisymmetric loading on the wing caused by the wing-fuselage interference. For a high-wing configuration, the induced loading would tend to increase the contribution of the upper-surface fins and to produce an equal and opposite effect on the lower-surface fins. The representation of the induced loadings presented in figure 9(b) indicates such an effect. At moderate angles of attack, the upper-surface fins were approximately 50 percent as effective as the lower-surface fins. At high angles of attack  $C_{n_{\psi}}$ , for the upper-surface fins, became less negative as the angle of attack was increased.

The value of the effective dihedral parameter  $C_{l_{\psi}}$  at  $\alpha=0^{\circ}$ , obtained with the upper-surface fins, was approximately the same as that obtained with the lower-surface fins (figs. 5 and 6). Consideration of the loads acting on the wing (fig. 9(b)) indicates that, since the addition of lower-surface fins at 0.70b/2 made  $C_{l_{\psi}}$  more positive (fig. 5), the addition of upper-surface fins at the same spanwise station should make  $C_{l_{\psi}}$  less positive, relative to the  $C_{l_{\psi}}$  of the basic configuration  $W_2$  + F +  $W_3$ . This apparent contradiction of the data can

be explained by accounting for the effects of the loading on the fins as well as the loading on the wing. The load on the lower-surface fins produced little rolling moment since the center of pressure of the load was approximately in the plane of the roll axis. The load on the uppersurface fins, however, produced a positive rolling moment (for positive angles of yaw) since the center of pressure of the load was above the roll axis.

The effective dihedral  $C_{l\psi}$  was positive throughout the angle-of-attack range for the twin upper-surface fin configuration. The fact that  $C_{l\psi}$  generally changes sign is attributed to the stalling of the wing tips. The fact that for this case  $C_{l\psi}$  did not change sign might have been due to the delay of the stall inboard of the fins, or possibly to the fact that the increment in positive  $C_{l\psi}$  produced by the load on the fins was large enough to compensate for the effects of wing-tip stall.

Basic configuration with wing fins and small fuselage fin. - A study of the directional stability characteristics of the model with twin fins generally showed low directional stability at low angles of attack but reasonably high stability at moderate and high angles of attack. The high-wing, single-vertical-tail configuration of reference 2 had a large amount of directional stability at low angles of attack but was unstable at moderate angles of attack (fig. 4). It appeared, therefore, that a combination of the best features of each type of fin arrangement would be desirable. Several combinations of twin vertical wing fins and a small vertical fin on the fuselage therefore were tested on the basic configuration, and the results are shown in figure 7. A comparison of these results with those of figures 5 and 6 indicates that the addition of the small fuselage fin produced a small increase in directional stability at low angles of attack and a small decrease in directional stability at the high angles of attack. This decrease in directional stability at high angles of attack may be attributed to the unfavorable sidewash at the small fuselage fin. None of the other aerodynamic parameters were affected appreciably by the addition of the small fuselage fin.

# Yawing Stability Characteristics

Basic configuration without vertical fins. The basic configuration  $W_2 + F + H_3$  had very little damping in yaw (negative  $C_{n_T}$ ) as shown in figure 8.

The negative value of  $C_{lr}$  obtained at  $\alpha=0^{\circ}$  can be accounted for by studying figure 9(c). The direction of the lateral component of the air flow at the wing-fuselage juncture depends, for the yawing-flow case, on the location of the juncture with respect to the center of gravity (or origion of axes). With the juncture ahead of the center of gravity (as for the present configuration), the lateral-velocity component is in the negative direction (negative angle of yaw) for positive yawing. Therefore, the induced loading on the wing, due to the wing-fuselage interference, produces a negative increment in rolling moment. This effect is opposite from that caused by a positive yaw angle (fig. 9(a)).

Basic configuration with vertical fins.— The contribution to the damping-in-yaw parameter  $C_{n_{\Gamma}}$  of the twin upper-surface and lower-surface fin configurations was approximately the same at low and moderate angles of attack (fig. 8). At the higher angles of attack, the damping in yaw for the upper-surface fins decreased rapidly with change in angle of attack, whereas the damping in yaw for the lower-surface fins did not decrease appreciably. A decrease in damping in yaw is signified by a less negative value of  $C_{n_{\Gamma}}$ . In general, the induced loadings caused by the vertical fins resulted in variations of  $C_{l_{\Gamma}}$  which were similar to the variations of  $C_{l_{\Gamma}}$  and, therefore, are not discussed.

The addition of a small fuselage fin to the twin upper-surface and lower-surface fin configurations had a negligible effect on  $\mathrm{C}_{lr}$  and  $\mathrm{C}_{Yr}$ . The main contribution of the small fuselage fin was to increase the damping in yaw slightly for both twin-fin configurations.

#### CONCLUSIONS

The results of an investigation of the low-speed static and yawing stability characteristics of a 45° sweptback high-wing, low-horizontal-tail model with various twin vertical wing fins indicate the following conclusions:

l. The directional-stability parameter  $C_{n_{\psi}}$  for a high-wing configuration with twin vertical fins placed either above or below the wing at about 70 percent of the wing semispan was found to be less negative at low angles of attack than for a similar configuration with only a single vertical tail at the rear of the fuselage. The twin-fin configurations, however, were directionally stable throughout the angle-of-attack range, whereas the single-vertical-tail configuration was directionally unstable at moderate and high angles of attack.

2. The twin upper-surface fin configuration was found to be more directionally stable at low angles of attack but only about 50 percent as effective as the twin lower-surface fin configuration at moderate angles of attack. At high angles of attack, the directional stability for the upper-surface fin configuration decreased as the angle of attack was increased.

- 3. The positive effective dihedral (at 0° angle of attack) normally associated with a high-wing fuselage configuration was increased by the addition of twin lower-surface fins at 70 percent of the wing semispan. As the lower-surface fins were moved outboard, the effective dihedral was reduced. With the fins mounted at the wing tips, the effective dihedral of the complete configuration was reduced to zero at 0° angle of attack. In the case of the upper-surface wing fins, the effective-dihedral parameter  $C_{l\psi}$  of the complete configuration was made more positive throughout the angle-of-attack range.
- 4. A small vertical fin placed at the rear of the fuselage produced a small increase in directional stability at low angles of attack for both the upper-surface or lower-surface wing-fin configuration. At high angles of attack, however, the small vertical fin tended to decrease the directional stability of both configurations.
- 5. The contribution of the upper-surface or lower-surface fins to the damping-in-yaw parameter  $C_{n_{\Gamma}}$  was approximately the same at low and moderate angles of attack. At the higher angles of attack, however, the damping in yaw contributed by the upper-surface fins tended to decrease as the angle of attack was increased.
- 6. In general, the static longitudinal stability was not affected by the upper-surface or lower-surface fins.

Langley Aeronautical Laboratory
National Advisory Committee for Aeronautics
Langley Field, Va., August 6, 1951

#### REFERENCES

- 1. Lichtenstein, Jacob H.: Effect of Horizontal-Tail Location on Low-Speed Static Longitudinal Stability and Damping in Pitch of a Model Having 45° Sweptback Wing and Tail Surfaces. NACA TN 2381, 1951.
- 2. Goodman, Alex: Effects of Wing Position and Horizontal-Tail Position on the Static Stability Characteristics of Models with Unswept and 45° Sweptback Surfaces with Some Reference to Mutual Interference. NACA TN 2504, 1951.
- 3. Schlichting, H.: Aerodynamics of the Mutual Influence of Aircraft Parts (Interference). Library Translation No. 275, British R.A.E., Oct. 1948.
- 4. Silverstein, Abe, and White, James A.: Wind-Tunnel Interference with Particular Reference to Off-Center Positions of the Wing and to the Downwash at the Tail. NACA Rep. 547, 1936.
- 5. Herriot, John G.: Blockage Corrections for Three-Dimensional-Flow Closed-Throat Wind Tunnels, with Consideration of the Effect of Compressibility. NACA Rep. 995, 1950. (Formerly NACA RM A7B28.)
- 6. Munk, Max M.: The Aerodynamic Forces on Airship Hulls. NACA Rep. 184, 1924.

# TABLE I.- PERTINENT GEOMETRIC CHARACTERISTICS OF MODEL

Fuselage:									
0									
Length, in									41.38
Fineness ratio									6.90
Wing:									
Aspect ratio, $A_W$									. 4.0
Taper ratio, $\lambda_{\text{W}}$									. 0.6
Quarter-chord sweep angle, deg						Wan J			. 45
Dihedral angle, deg									. 0
Twist, deg									. 0
NACA airfoil section									65A008
Area, Sw, sq in									324.0
Span, b, in									36.0
Mean aerodynamic chord, $\overline{c}_W$ , in.									9.19
Wing height, $Z_W$ , in									2.00
Wing-height retio 7-1d				•				•	
Wing-height ratio, $Z_W/d$								•	0.333
Horizontal tail:									
									. 4.0
Aspect ratio, A <sub>H</sub>								•	
Taper ratio, $\lambda_{\mathrm{H}}$								•	. 0.6
Quarter-chord sweep angle, deg									. 45
Dihedral angle, deg									. 0
Twist, deg				•				•	. 0
NACA airfoil section									65A008
Area, S <sub>H</sub> , sq in									64.8
Span, b <sub>H</sub> , in									16.1
Mean aerodynamic chord, $\overline{c}_{H}$ , in.									4.11
Area ratio, $S_H/S_W$									0.20
Tail length, l <sub>H</sub> , in									19.25
Tail-length ratio, $l_{\rm H}/\bar{c}_{\rm W}$									2.09
Tail height, Z <sub>H</sub> , in									1.50
и потвиту, ин		•							1.00
Vertical tail:									
Aspect ratio, $A_{V}$									2.0
Taper ratio, $\lambda_V$									06
									0.0
Quarter-chord sweep angle, deg									0.6
Quarter-chord sweep angle, deg									45
Quarter-chord sweep angle, deg NACA airfoil section						: :	: :		45 65A008
Quarter-chord sweep angle, deg NACA airfoil section $\dots$ Area, $S_V$ , sq in. $\dots$	: :		: :		٠.		: :	:	45 65A008 48.6
Quarter-chord sweep angle, deg NACA airfoil section Area, $S_V$ , sq in						: :		:	45 65A008 48.6 9.86
Quarter-chord sweep angle, deg NACA airfoil section $\dots$ Area, $S_V$ , sq in. $\dots$						: :		:	45 65A008 48.6
Quarter-chord sweep angle, deg NACA airfoil section Area, $S_V$ , sq in								:	45 65A008 48.6 9.86 16.70
Quarter-chord sweep angle, deg NACA airfoil section Area, $S_V$ , sq in			: :			· · ·		:	45 65A008 48.6 9.86
Quarter-chord sweep angle, deg NACA airfoil section						· · ·		:	45 65A008 48.6 9.86 16.70
Quarter-chord sweep angle, deg NACA airfoil section						· · ·	1	:	45 65A008 48.6 9.86 16.70
Quarter-chord sweep angle, deg NACA airfoil section							1 .2		45 65A008 48.6 9.86 16.70 f <sub>2</sub> 1.7
Quarter-chord sweep angle, deg NACA airfoil section						f 1	1 .2 0 .3		45 65A008 48.6 9.86 16.70 f <sub>2</sub> 1.7
Quarter-chord sweep angle, deg NACA airfoil section						ff 1	1 .2 0 .3		45 65A008 48.6 9.86 16.70 f <sub>2</sub> 1.7 0 51.3
Quarter-chord sweep angle, deg NACA airfoil section						ff 1	1 .2 0 .3 See		45 65A008 48.6 9.86 16.70 f <sub>2</sub> 1.7 0 51.3 gure 2
Quarter-chord sweep angle, deg NACA airfoil section						f 1 51 30	1 .2 0 ·3 See .0 .0		45 65A008 48.6 9.86 16.70 f <sub>2</sub> 1.7 0 51.3 gure 2 38.0
Quarter-chord sweep angle, deg NACA airfoil section						ff 1 51 30 6	1 .2 0 ·3 See .0 .0		45 65A008 48.6 9.86 16.70 f <sub>2</sub> 1.7 0 51.3 gure 2 38.0 8.0
Quarter-chord sweep angle, deg NACA airfoil section Area, S <sub>V</sub> , sq in.  Span, b <sub>V</sub> , in.  Tail length, l <sub>V</sub> , in.  Upper-surface and lower-surface fins: Aspect ratio, A <sub>f</sub> Taper ratio, λ <sub>f</sub> Quarter-chord sweep angle, deg Airfoil section Area, S <sub>f</sub> , sq in.  Span, b <sub>f</sub> , in.  Fin length, l <sub>f</sub> , in. at 0.70b/2  Rear vertical fin:						ff 1 51 30 6	1 .2 0 ·3 See .0 .0		45 65A008 48.6 9.86 16.70 f <sub>2</sub> 1.7 0 51.3 gure 2 38.0 8.0
Quarter-chord sweep angle, deg NACA airfoil section Area, S <sub>V</sub> , sq in. Span, b <sub>V</sub> , in. Tail length, l <sub>V</sub> , in.  Upper-surface and lower-surface fins: Aspect ratio, A <sub>f</sub> Taper ratio, λ <sub>f</sub> Quarter-chord sweep angle, deg Airfoil section Area, S <sub>f</sub> , sq in. Span, b <sub>f</sub> , in. Fin length, l <sub>f</sub> , in. at 0.70b/2  Rear vertical fin: Aspect ratio, A <sub>V</sub>						ff 1 51 30 6	1 .2 0 ·3 See .0 .0		45 65A008 48.6 9.86 16.70 f <sub>2</sub> 1.7 0 51.3 gure 2 38.0 8.0
Quarter-chord sweep angle, deg NACA airfoil section Area, S <sub>V</sub> , sq in. Span, b <sub>V</sub> , in. Tail length, l <sub>V</sub> , in.  Upper-surface and lower-surface fins: Aspect ratio, A <sub>f</sub> Taper ratio, λ <sub>f</sub> Quarter-chord sweep angle, deg Airfoil section Area, S <sub>f</sub> , sq in. Span, b <sub>f</sub> , in. Fin length, l <sub>f</sub> , in. at 0.70b/2  Rear vertical fin: Aspect ratio, λ <sub>V</sub> Taper ratio, λ <sub>V</sub>						ff 1 51 30 6	1 .2 0 ·3 See .0 .0		45 65A008 48.6 9.86 16.70 f <sub>2</sub> 1.7 0 51.3 gure 2 38.0 8.0 9.4
Quarter-chord sweep angle, deg NACA airfoil section Area, Sy, sq in.  Span, by, in.  Tail length, ly, in.  Upper-surface and lower-surface fins: Aspect ratio, Af Taper ratio, Af Quarter-chord sweep angle, deg Airfoil section Area, Sf, sq in.  Span, bf, in.  Fin length, lf, in. at 0.70b/2  Rear vertical fin: Aspect ratio, Ay Taper ratio, Ay Quarter-chord sweep angle, deg						ff 1 51 30 6	1 .2 0 ·3 See .0 .0		45 65A008 48.6 9.86 16.70 f <sub>2</sub> 1.7 0 51.3 gure 2 38.0 8.0 9.4
Quarter-chord sweep angle, deg NACA airfoil section Area, Sy, sq in. Span, by, in. Tail length, ly, in.  Upper-surface and lower-surface fins: Aspect ratio, Af Taper ratio, Af Quarter-chord sweep angle, deg Airfoil section Area, Sf, sq in. Span, bf, in. Fin length, lf, in. at 0.70b/2  Rear vertical fin: Aspect ratio, Ay Taper ratio, Ay Quarter-chord sweep angle, deg Airfoil section						ff 1 300 66 99	 1.2 0.3 See	fi	45 65A008 48.6 9.86 16.70 f <sub>2</sub> 1.7 0 51.3 gure 2 38.0 8.0 9.4
Quarter-chord sweep angle, deg NACA airfoil section Area, Sy, sq in. Span, by, in. Tail length, ly, in.  Upper-surface and lower-surface fins: Aspect ratio, Af Taper ratio, Af Quarter-chord sweep angle, deg Airfoil section Area, Sf, sq in. Span, bf, in. Fin length, lf, in. at 0.70b/2  Rear vertical fin: Aspect ratio, Av Taper ratio, Av Quarter-chord sweep angle, deg Airfoil section Area, Sy, sq in.						ff 1 300 66 99	 1.2 0.3 See	fi	45 65A008 48.6 9.86 16.70 f <sub>2</sub> 1.7 0 51.3 gure 2 38.0 8.0 9.4
Quarter-chord sweep angle, deg NACA airfoil section Area, Sy, sq in. Span, by, in. Tail length, ly, in.  Upper-surface and lower-surface fins: Aspect ratio, Af Taper ratio, Af Quarter-chord sweep angle, deg Airfoil section Area, Sf, sq in. Span, bf, in. Fin length, lf, in. at 0.70b/2  Rear vertical fin: Aspect ratio, Av Quarter-chord sweep angle, deg Airfoil section Area, Sy, sq in. Span, by, in.						ff 1 30 66 9	 1.2 0.3 See	fi	45 65A008 48.6 9.86 16.70 f <sub>2</sub> 1.7 0 51.3 gure 2 38.0 8.0 9.4 0.84 0 60.7 gure 2
Quarter-chord sweep angle, deg NACA airfoil section Area, Sy, sq in. Span, by, in. Tail length, ly, in.  Upper-surface and lower-surface fins: Aspect ratio, Af Taper ratio, Af Quarter-chord sweep angle, deg Airfoil section Area, Sf, sq in. Span, bf, in. Fin length, lf, in. at 0.70b/2  Rear vertical fin: Aspect ratio, Av Quarter-chord sweep angle, deg Airfoil section Area, Sy, sq in. Span, by, in.						ff 1 30 66 9	 1.2 0.3 See	fi	45 65A008 48.6 9.86 16.70 f <sub>2</sub> 1.7 0 51.3 gure 2 38.0 8.0 9.4 0.84 0 60.7 gure 2 19.0
Quarter-chord sweep angle, deg NACA airfoil section Area, Sy, sq in. Span, by, in. Tail length, ly, in.  Upper-surface and lower-surface fins: Aspect ratio, Af Taper ratio, Af Quarter-chord sweep angle, deg Airfoil section Area, Sf, sq in. Span, bf, in. Fin length, lf, in. at 0.70b/2  Rear vertical fin: Aspect ratio, Av Taper ratio, Av Quarter-chord sweep angle, deg Airfoil section Area, Sy, sq in.						ff 1 30 66 9	 1.2 0.3 See	fi	45 65A008 48.6 9.86 16.70 f <sub>2</sub> 1.7 0 51.3 gure 2 38.0 8.0 9.4 0.84 0 60.7 gure 2 19.0 4.0

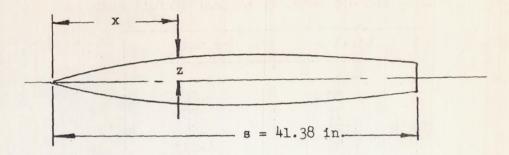
TABLE II. - ORDINATES FOR NACA 65A008 AIRFOIL

Station and ordinates in percent airfoil chord

Station	Ordinate		
0 .75 1.25 2.50 5.0 7.5 10.0 15 20 25 30 35 40 45 50 55 60 65 70 75 80 85 90 95 100	0 .62 .75 .95 1.30 1.75 2.12 2.43 2.93 3.30 3.59 3.79 3.93 4.00 3.99 3.90 3.71 3.46 3.14 2.76 2.35 1.90 1.43 .96 .49 .02		
L.E. radius 0.408			

NACA

TABLE III. - FUSELAGE ORDINATES



x/s	z/s
0	0
.025	.007
.050	.014
.075	.020
.100	.026
.125	.032
.15	.038
.20	.048
.25	.056
.30	.062
.35	.066
.40	.0715
.45	.0724
.50	.0720
.55	.0710
.60	.068
.65	.065
.70	.061
.75	.056
.80	.051
.85	.045
.90	.032

NACA

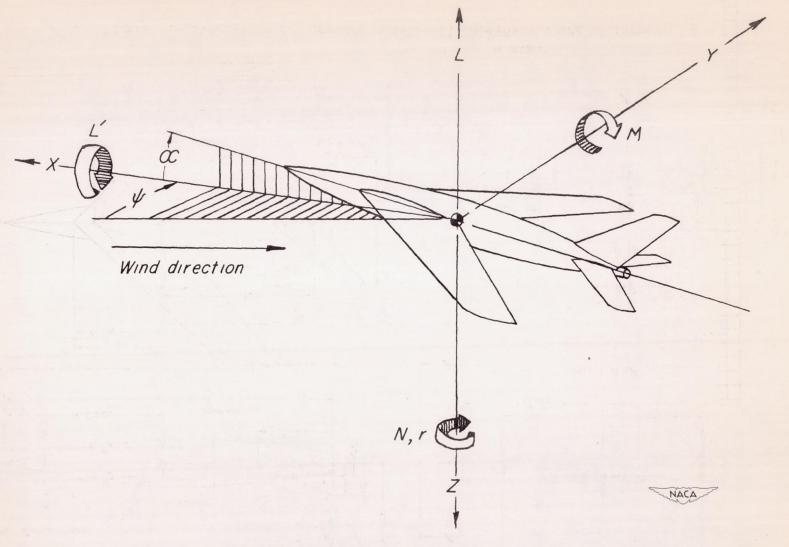


Figure 1.- System of axes used. Arrows indicate positive directions of angles, forces, and moments.

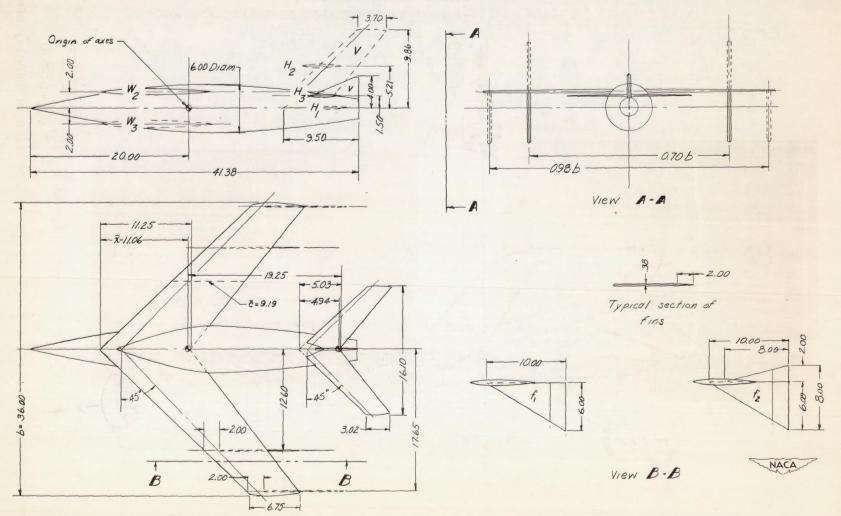
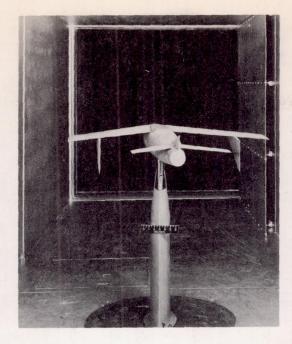
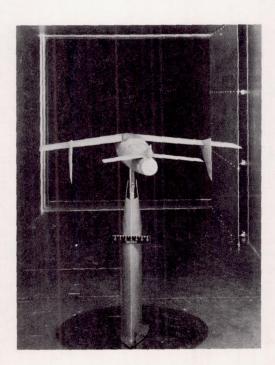


Figure 2.- Dimensions of complete model. All dimensions are in inches.



(a)  $W_2 + F + H_3 + v + f_1$  at  $0.70\frac{b}{2}$ . L-68799



(b)  $W_2 + F + H_3 + v_1 + f_2$  at  $0.70\frac{b}{2}$ . L-68800

Figure 3.- Models mounted in 6- by 6-foot test section of Langley stability tunnel.

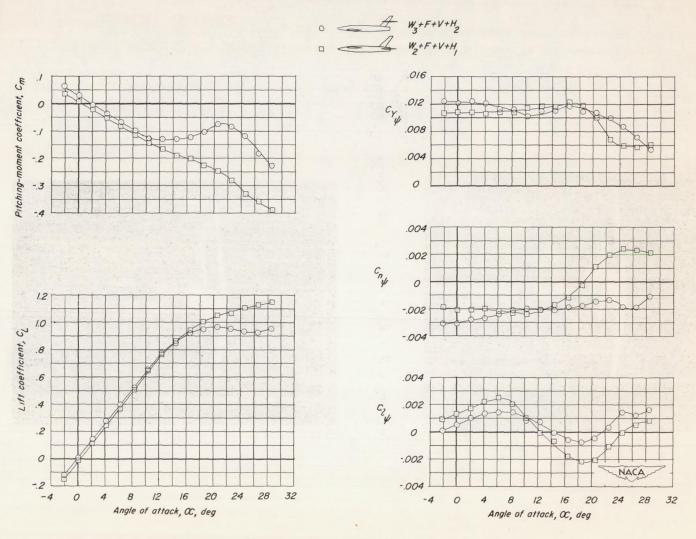


Figure 4.- Comparison of the static stability characteristics of a low-wing, high-horizontal-tail configuration and a high-wing, low-horizontal-tail configuration (data from reference 2).

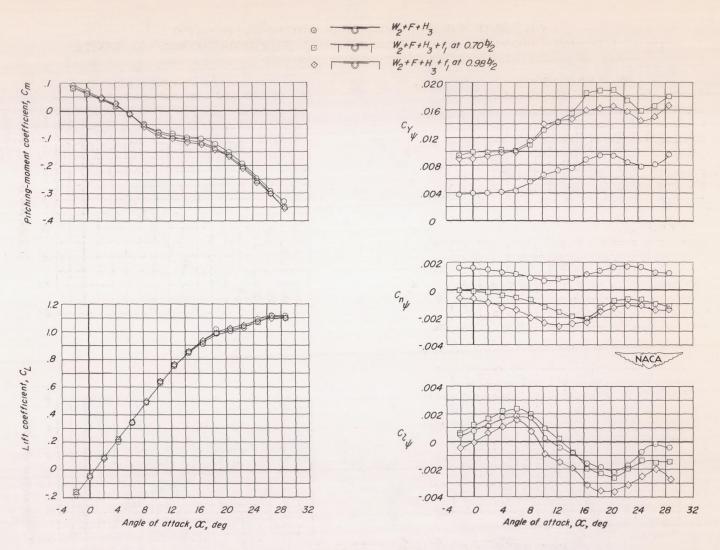


Figure 5.- Static stability characteristics of a high-wing, low-horizontaltail configuration with twin lower-surface wing fins located at two spanwise stations.

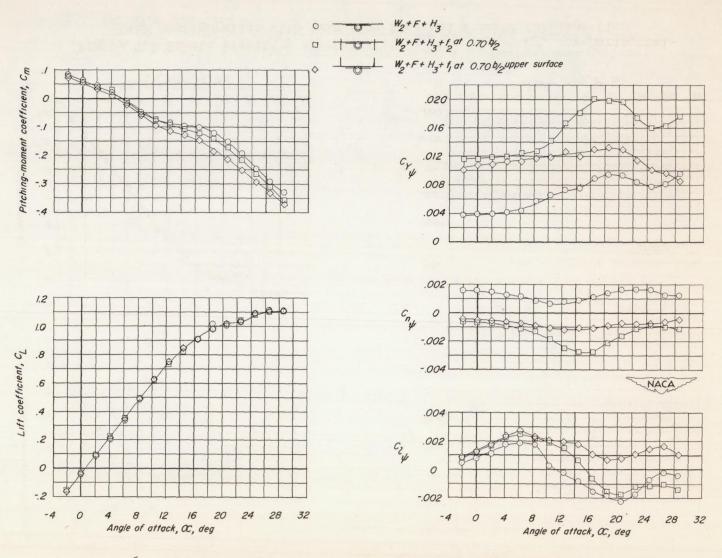


Figure 6.- Static stability characteristics of a high-wing, low-horizontal-tail configuration with upper-surface wing fins.

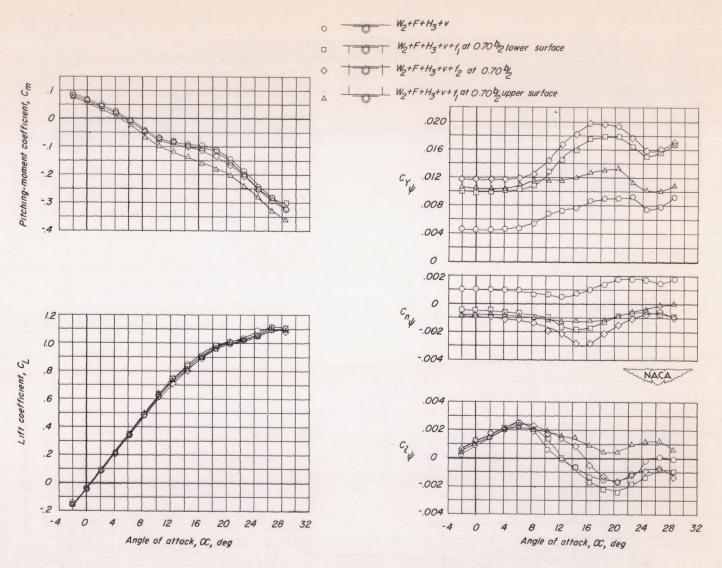


Figure 7.- Static stability characteristics of a high-wing, low-horizontal-tail configuration with twin wing fins and a small fuselage fin.

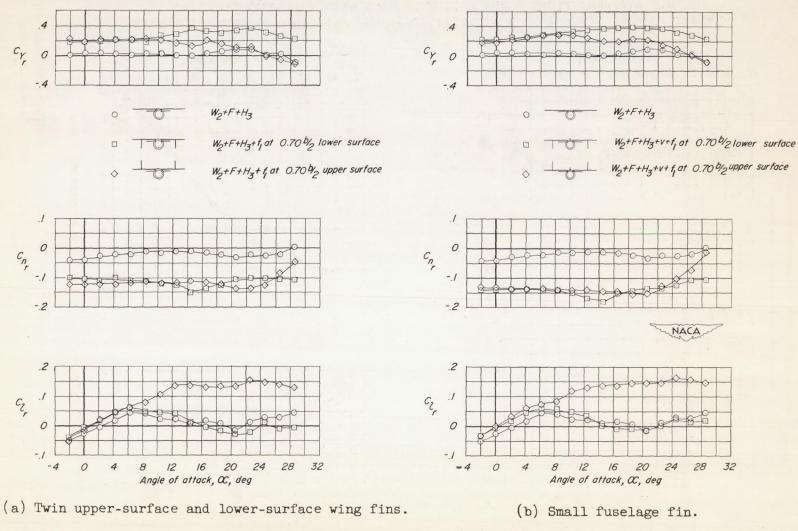
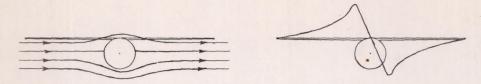


Figure 8.- Yawing stability characteristics of a high-wing, low-horizontal-tail configuration.

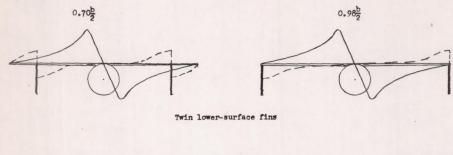
4

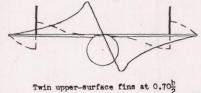
Loads caused by wing-fuselage interference

Loads caused by wing-fin interference

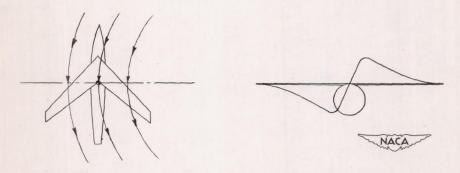


(a) High-wing configuration at a positive angle of yaw (rear view of model).





(b) High-wing configuration with twin upper-surface and lower-surface wing fins (rear view of model).



(c) High-wing configuration in yawing flow.

Figure 9.- Representation of loads induced on wing by wing-fuselage and wing-fin interferences at a positive angle of yaw. Areas between wing and curves represent lift.